

# **CHAPTER ONE**

## **INTRODUCTION**

## 1.1 Preface:

Worldwide Interoperability for Microwave Access (WiMAX) network was developed to allow users to have high-speed broadband internet access at speeds equivalent to cable/DSL and the same mobility provided by the cellular network simultaneously. WiMAX is a broadband wireless network that combines the fixed broadband and mobile cellular network into one flexible and easily deployable Network.

In communication system many techniques, like Frequency Division Multiplexing Access (FDMA), Time Division multiplexing Access (TDMA) and Code Division Multiplexing Access (CDMA), are used for transmission of signal. Where FDMA has very bad spectrum usage and TDMA performance degrades by multipath delay spread causing Inter Symbol Interference (ISI). In contrast OFDM enables high bit-rate wireless applications in a multipath radio environment the need for complex receivers. OFDM is a multi-channel modulation system employing Frequency Division Multiplexing (FDM) of orthogonal sub-carriers, each modulating a low bit-rate digital stream.

Channel estimation is an important issue in any OFDM-based system for demodulation and decoding. In general, an OFDM waveform can be viewed as a two-dimensional (2D) lattice in the time-frequency plane. For pilot-assisted channel estimation techniques, where pilots refer to reference signals known at both transmitter and receiver, this 2D lattice can be viewed as being sampled at the pilot positions, and the channel characteristics between pilots are estimated by interpolation. The two basic aspects of OFDM channel estimation are the arrangement of pilot positions, and the design of the channel estimator to interpolate between the pilots. The goal in designing channel estimators is to solve

this problem with a satisfactory trade-off between complexity and performance.

## **1.2 Problem Definition:**

A problem with any communication system is that its data rate can be limited by distortion caused by the channel. To mitigate the effect of the channel, the receiver must perform channel estimation to remove this distortion. The task of channel estimation is made more difficult in a wireless environment because the channel is fast-changing and unpredictable. Because of this, good channel estimators are required to accurately estimate the channel while minimizing the amount of time, data, and computations necessary to do so.

There are two main problems in designing channel estimators for wireless OFDM systems.

- 1- The arrangement of pilot information, where pilot means the reference signal used by both transmitters and receivers.
- 2- The design of an estimator with both low complexity and good channel tracking ability and the two problems are interconnected.

## **1.3 Proposed Solutions:**

In order to estimate the effect of the channel, the position of pilot information must be in appropriate form so the estimation will be more effective. So we must choose the arrangement of pilot in which the position of each pilot is sort to be between a certain numbers of data subcarriers. So the arrangement of pilots and data subcarriers will be regular.

To design an estimator that has low complexity of computation and better performance we used LS estimation algorithm.

#### **1.4 Aim and Objectives:**

The aim of this study is to improving channel estimation in uplink WiMAX system, which is based on OFDM, because channel state information is required for signal detection at receiver and its accuracy affects the overall performance of system and it is essential to improve the channel estimation for more reliable communications.

Our objectives will be focuses on:

- To analyze the performance of uplink channel estimation algorithms that can be used in Partial Usage of Sub-carriers (PUSC).
- To analyze the performance of uplink channel estimation algorithms that can be used in Adaptive Modulation and coding (AMC).
- To compare between these algorithms and decide which one is more effective in term of complexity computation and better performance.

## **1.5 Methodology:**

In this study we will spot the light on the channel estimation in the mobile WiMAX networks. To do that we have to apply some of the algorithms that is used to implement channel estimation techniques, and MATLAB will be the main tool that we will use it.

First the estimation methods in case of PUSC permutation mode are introduced and a comparison between it are made. Then the estimation methods in AMC permutation mode are compared between each one of them. From the relationship between SNR and MSE, we can decide which algorithm is better in a certain SNR.

## **1.6 Thesis Outline:**

The organization of this research is as follows:

- Chapter 2, provides more detailed description of WiMAX and some of the theory behind OFDM. In addition, the old studies on channel estimation in OFDM systems including WiMAX, will be reviewed in this chapter and some background on the previous work in this field.
- Chapter 3, covers the channel estimation in PUSC and AMC permutation modes in WiMAX, illustration and analyzing of two algorithms in each mode under different conditions.
- Chapter 4, contains the simulation results on each of the algorithms and briefly summarized it.

- Chapter 5, is about demonstrate and summarizing the conclusions from this study.

## **CHAPTER TWO**

### **BACKGROUND**

## **2.1 Introduction:**

Channel estimation has received a lot of attention in recent years because of its importance in wireless communications. Without a good channel estimator, the throughput and coverage of the wireless system is severely limited. OFDM has become very popular in wireless communication systems including WiMAX because of it has many advantages over other techniques, such as: resistance to multipath channel fading and simple channel equalizer, resistance to narrow band interference, and its permits high data rate compared with FDM, so a lot of research work has been placed in designing a good channel estimator for OFDM systems.

### **2.1.1 IEEE 802.16 WiMAX Standard:**

WiMAX (Worldwide Interoperability for Microwave Access) is an emerging technology in wireless communications and will play a major role in broadband wireless metropolitan networks. WiMAX stands for Worldwide Interoperability for Microwave Access and is based on the IEEE 802.16 (Wireless MAN) standard.

When the IEEE 802.16 standard was initially released in 2001, the only specifications defined were for the 10-66GHz range and targeted wireless networks where line of sight was present. However, in 2004, the specification was amended to revision D (IEEE 802.16d) to include the 2-11GHz frequency band where fixed and low mobility environments could be supported. In 2005, an amendment was added and the IEEE 802.16e standard was created to support full mobility and included



features such as MIMO and Scalable OFDMA. In general, WiMAX refers to networks that meet specifications in the IEEE 802.16d and/or IEEE 802.16e revision of the standard. WiMAX defines profiles" which are composed of a subset specifications from the 802.16d and 802.16e standard that vendors can use to certify their products [1].

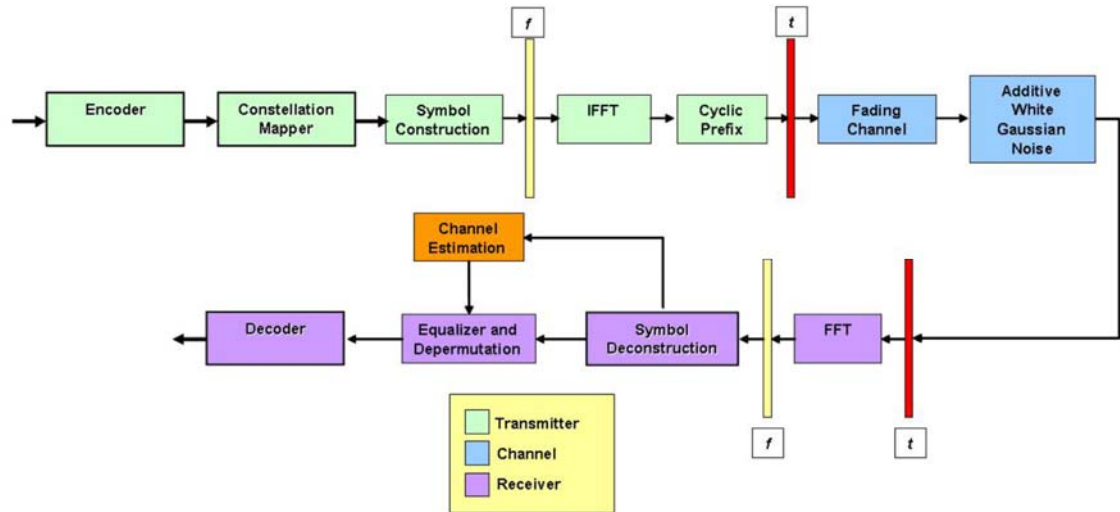


**Figure 2.1: WiMAX System Level Block Diagram**

WiMAX is also an OFDM-based system, but unique in that it employs OFDMA (Orthogonal Frequency Division Multiple Access) which is the multi-user version of OFDM. The difference between WiMAX and other OFDM systems is that it allows multiple users to simultaneously access the channel by allocating a different set of sub-channels to each user. This extra degree of freedom allows WiMAX to exploit the frequency-selective channel by allocating sub-channels to users with favourable conditions in those sub-channels and/or avoid allocating sub-channels to users in which their channel conditions are poor. However, this unique feature also makes channel estimation in

WiMAX more difficult because fewer subcarriers can be used in estimating the channel[2].

### **2.1.2 Mobile WiMAX:**

Mobile WiMAX is a rapidly growing broadband wireless access technology based on IEEE 802.16d-2004 and IEEE 802.16e-2005 air-interface standards. The WiMAX forum is developing mobile WiMAX system profiles that define the mandatory and optional features of the IEEE standard that are necessary to build a mobile WiMAX compliant air interface which can be certified by the WiMAX Forum. Mobile WiMAX is not the same as IEEE 802.16e-2005, rather a subset of the IEEE STD 802.16 standard features and functionalities.

The WiMAX Forum Network Working Group (NWG) is developing the higher-level networking specifications for Mobile WiMAX systems beyond what is defined in the IEEE 802.16 standard that simply addresses the air interface specifications. The combined effort of IEEE 802.16 and the WiMAX Forum help define the end-to-end system solution for a Mobile WiMAX network[3].

## **2.2 Background of Channel Estimation:**

In order to make any decision as to which solution is best fit to fulfil the given requirements it was necessary to establish a foundation on which to base a discussion. Channel estimation in OFDM systems is the base of channel estimation in WiMAX networks, hence available

methodologies and algorithms will be investigated through a following literature review.

### **2.2.1 Review of OFDM Estimators:**

Over all oldest studies the focus was on how to implement an effective Algorithms for channel estimation compromising between complexity and performance , among many algorithms have been implemented and applied we will focus on three algorithms , briefly highlight them , and comparing between them . These algorithms are:

- 1- LS Channel Estimation
- 2- MMSE Channel Estimation
- 3- Linear Interpolation Channel Estimation

#### **2.2.1.1 OFDM System Description:**

Paper [4] state that the OFDM transmission scheme makes it easy to assign pilots in both time and frequency domain. Figure 2.2 shows two major types of pilot arrangement. The first kind of pilot arrangement shown in Figure.2a is denoted as block-type pilot arrangement. The pilot signal is assigned to a particular OFDM block, which is sent periodically in time domain. This type of pilot arrangement is especially suitable for slow-fading radio channels. The estimation of channel response is usually obtained by either LS or MMSE estimates of training pilots. The second kind of pilot arrangement, shown in Figure. 2b is denoted as comb-type pilot arrangement. The pilot signals are uniformly distributed within each OFDM block. Assuming that the payloads of pilot signals of

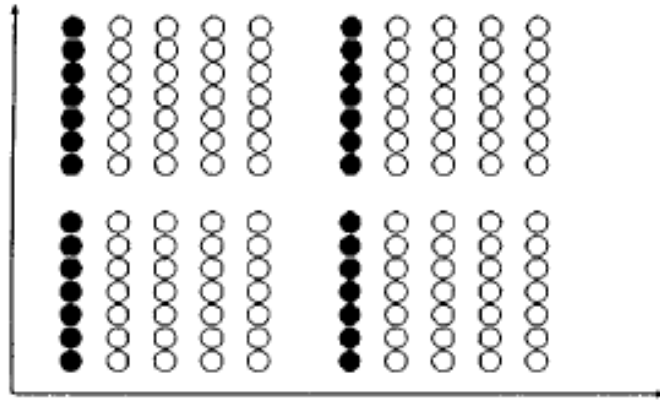
the two arrangements are the same, the comb-type pilot assignment has a higher retransmission rate.

Thus, the comb-type pilot arrangement system is provides better resistance to fast-fading channels. Since only some sub-carriers contain the pilot signal, the channel response of no pilot subcarriers will be estimated by interpolating neighboring pilot sub- channels. Thus, the comb-type pilot arrangement is sensitive to frequency selectivity when comparing to the block-type pilot arrangement system.

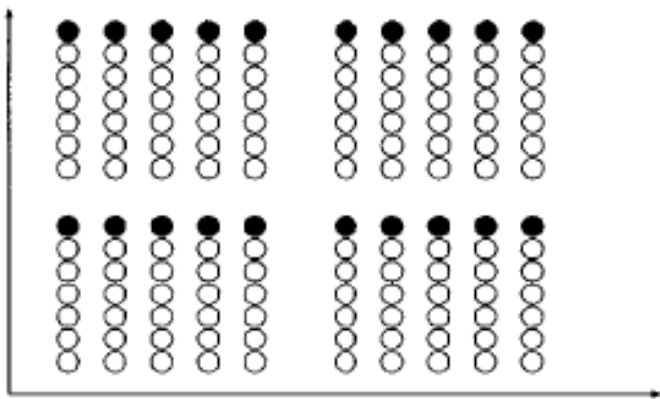
That is, the pilot spacing  $(\Delta f)_p$ , must be much smaller than the coherence bandwidth of the channel  $(\Delta f)_c$ .

### **2.2.1.2 LS Channel Estimation Algorithm:**

PK Pradhan and others [3],found that the LS estimate of pilot signal is susceptible to Additive White Gaussian Noise (AWGN) and Inter-Carrier Interference (ICI). Because the channel responses of data subcarriers are obtained by interpolating the channel characteristics of pilot subcarriers, the performance of OFDM systems which are based on comb-type pilot arrangement is highly dependent on the rigorousness of estimate of pilot signals. Thus, another estimate better than the LS estimate is required.



- ❖ **Comb Type**
- ❖ **Some sub-carriers are reserved for pilots for each symbol.**



- ❖ **Block Type**
- **All sub-carriers reserved for pilots with a specific period**

**Figure 2.2: Pilot Arrangement Types**

### **2.2.1.3 MMSE Channel Estimation Algorithm:**

The minimum mean-square error is widely used in the OFDM channel estimation since it is optimum in terms of mean square error

(MSE) in the presence of AWGN[5]. In fact, it is observed in the work of Athaudage and Jayalath[6], that many channel estimation techniques are indeed a subset of MMSE channel estimation technique. The MMSE estimator employs the second-order statistics of the channel, channel correlation function, and the operating SNR.

The above MMSE estimator according to J Hwang[7] yields much better performance than LS estimator, especially under the low SNR scenarios. However, a major drawback of the MMSE estimator is its high computational complexity and it increases exponentially as the number of carrier increases [4].

Another drawback of this estimator is that it requires one to know the correlation of the channel and the operating SNR in order to minimize the MSE between the transmitted and received signals. However, in wireless links, the channel statistics depend on the particular environment, for example, indoor or outdoor, Line-Of-Sight (LOS) or Non-Line-Of-Sight(NLOS), and changes with time. Therefore, MMSE estimator may not be feasible in a practical system[7].

#### **2.2.1.4 Linear Interpolation Channel Estimation Algorithm:**

Linear interpolation is the simplest method to estimate channel from raw channel estimates at pilot frequencies. This is done by linearly interpolating the raw channel estimates at the two nearest pilot sub-carriers. Although linear interpolation provides some limited noise reduction of the channel estimates at data locations, it is the simplicity of

the solution that is attractive. Some additional gain may be obtained by averaging the interpolated channel estimates using a sliding window.

We note that averaging window length (number of used pilots in window) is inversely proportional to the coherence bandwidth of the channel. For a channel with high frequency coherence bandwidth (small excess delay), a large number of interpolated channel coefficients may be used for averaging and vice versa. We note that other options exist for interpolation-based methods such as Gaussian interpolation filters and cubic spline interpolation filters[8].

### **2.2.2 Review of WiMAX Estimators:**

WiMAX supports a wide variety of applications ranging from voice services that are latency-sensitive to real-time multimedia services where a consistent high data throughput must be maintained. In addition, users may be using any one of these services while walking or riding in a car where the wireless channel appears to be fast-changing to the receiver. Because of these requirements, it is particularly important that a WiMAX channel estimator be designed to be both fast and accurate. And while WiMAX is an OFDM-based system, channel estimation is more difficult in WiMAX than traditional OFDM systems because the estimator has fewer sub-carriers to use [2].

#### **2.2.2.1 Sub-Channelization:**

To allow multiple accesses to the channel, WiMAX uses two types of subcarrier allocation modes or permutations: Distributed and Adjacent. A distributed subcarrier permutation pseudo randomly

allocates subcarriers to sub-channels to exploit frequency diversity. Partial Usage of Subcarriers (PUSC) is one example of a distributed subcarrier permutation.

An adjacent subcarrier permutation forms sub-channels of adjacent subcarriers and leaves the responsibility of determining the optimum allocation to the scheduler. Adaptive Modulation and Coding (AMC) is one example of an adjacent subcarrier permutation. In AMC, channel sounding is an optional feature sometimes used to aid the base station in determining each user's unique channel condition. This technique is implemented by reserving OFDM symbols typically at the end of the uplink frame for users to transmit known sounding sequences for the base station to use to estimate the channel of each user in the system[2].

### **OFDM vs. WiMAX:**

There are several methods of channel estimation in uplink WiMAX system have been studied through the past decade, in[9]the authors stated that in WiMAX systems standardized by IEEE-SA Standards Board (2005), a different transmission structure and corresponding arrangement of pilot positions are used to fully employ the diversities in both the time and the frequency dimensions. The subcarriers allocated to a subscriber are both separated in frequency and hopped periodically in time. This dynamic resource allocation scheme makes it unfeasible to employ second-order statistics in either the frequency or the time dimension for uplink channel estimation, in other words, it is unfeasible to apply traditional OFDM channel estimation algorithms to WiMAX systems. However, on the other hand, because channel estimation has been constrained inside a small basic transmission unit, 2D interpolation is tolerable in terms of computational complexity.



In pilot-based channel estimation techniques, reference signals known at both transmitter and receiver are transmitted periodically. The subcarriers allocated to a user are separated in frequency in any time slot, and change locations from slot-to-slot. This dynamic allocation scheme takes advantage of potential system diversities in both time and frequency, due to the expected de-correlation in both the time and frequency dimensions. For example, a deep narrow-band fade usually affects only a fraction of subcarriers in each sub-channel, and a deep long-term channel fade may affect a given user for only a short period of time due to the hopping. Also, this scheme provides better capacity performance than the traditional OFDM systems, due to the flexible user transmission start-time and duration of transmission length.

However, such a complicated allocation scheme makes accurate channel estimation difficult. It is often not feasible to use the channel correlation across tiles in the frequency dimension, because the tiles can be separated beyond the coherence bandwidth of the channel, and thus, the correlation is weak. It also might not be feasible to employ the channel correlation across tiles in the time dimension, because the locations of tiles change every time slot, and thus depending upon the channel coherence time, it might be difficult to track/ estimate the channel conditions. Based on the above considerations, channel estimation for uplink WiMAX systems can be effectively accomplished by using information within a single tile. This kind of estimation will experience less precision, because we can neither average across tiles nor employ second-order statistics of the channel (correlation, delay, etc.).

That is why a relatively large number of pilot bits (four out of twelve) is employed in the tile structure[9].

In the 2D averaging algorithm, the average of the four pilot subcarriers is used for the channel estimator for all the data subcarriers inside the tile.

This algorithm is a simple channel estimation technique for WiMAX systems. It is also efficient in reducing effects of noise, since the variance of noise will be reduced by a factor of 4. It is suitable for a channel where the fading is slow, and where the neighbouring frequency subcarriers are highly correlated [9]. This technique is used to overcome the effects of multipath fading since the wavelength for different frequencies result in different and uncorrelated fading characteristics.

The accuracy of this method depends mostly on the accuracy of estimated pilot data so that in order to improve the performance, we can use the enhanced linear estimator MMSE instead of LS estimator to estimated pilot data at the receiver [10].

The authors of [11]found that Kalman algorithm combining with guard interval optimization algorithm had better performance than LS with fixed GI. This is shown clearly in 16-QAM modulation. In addition, with all three modulations, we see that Kalman estimator with fixed GI is much better than LS estimator.

In 4-QAM modulation, BER parameter for two methods Kalman estimator and Kalman estimator combining with guard interval optimization algorithm are nearly equal when SNR is higher than 10db. Relatively [12]show that Extended Kalman Filter had the best

performance in indoor model and pedestrian model where mobile speed is smaller than 10 km/h.

### **2.2.2.2 Interpolation Algorithms Based on LS Channel**

#### **Estimation:**

There are two kinds of channel estimation algorithm in OFDM system according to [13], blind channel estimation and pilot-based channel estimation. The pilot-based channel estimation estimates the channel response according to the known information of the pilot tone; it is simple and has good performance.

The blind channel estimation does not need pilot; it can save the bandwidth but the performance is not so good. As the pilot tone is defined in the WiMAX system, the pilot-based channel estimation is used in most application. Generally, there are MMSE algorithm and LS algorithm for pilot-based channel estimation. The MMSE algorithm has better performance[14], but with higher complexity. The LS algorithm is relatively simple and with acceptable performance, so it is widely used. In LS channel estimation, the interpolation algorithm is very important; it affects the precision of the channel estimation and performance of the system.

Although different interpolations have different performance in different channel, the two order I-Q interpolation can get good performance in nearly all the channel with acceptable increasing of complexity, so it is advised to be used in practical application [9].

### **Bilinear Interpolation Algorithm:**

Another possible interpolation algorithm is bilinear interpolation where the data subcarrier are estimated by horizontal or vertical 1D linear interpolation, based upon fitting straight lines between the samples.

This algorithm will be appropriate if the channel is fast fading, and the neighbouring frequency bands are weakly correlated. Note that, because the input data used for interpolation have only 2 points in any given row or column[9].

### **Two Order I-Q Interpolation Algorithm:**

Two order I-Q interpolation algorithms calculates the channel response of the data subcarriers according to the channel information of 3 neighbouring pilot tone, the correlation of the channel is fully utilized.

The two order I-Q interpolation can get good performance in nearly all the channel with acceptable increasing of complexity; it is advised to be used in practical application [13].

### **DFT Interpolation:**

In DFT interpolation, the channel response  $\hat{H}_p$  at the pilot subcarrier is transformed by IDFT to  $\hat{h}_p$  in time domain, and then  $N - N_p$  zeroes are inserted into the middle of the  $\hat{h}_p$ , finally DFT transform is performed to get the channel response  $\hat{H}_p$  for all subcarrier. As fast algorithm can be used instead, the DFT interpolation can be also named FFT Interpolation[13].

### **Frequency-Averaging-Time-Interpolation (FATI) Algorithm:**

The frequency-averaging-time-interpolation (FATI) algorithm is a combination of the averaging algorithm and the bilinear interpolation algorithm. It functions by averaging in the frequency dimension and linearly interpolating in the time dimension.

This algorithm uses averaging in frequency that is suitable where the neighbouring frequency subcarriers are highly correlated, and uses interpolation in time that is suitable where the channel fading is relatively fast.

FATI algorithm is the best choice among them if the algorithm is designed for a system with unknown system parameters, because it has a relatively simple realization structure and relatively acceptable performance over a broad range of scenarios [9].

### **Time-Domain-Interpolation (TDI) Algorithm:**

In the time-domain-interpolation (TDI) algorithm, a DFT-based frequency interpolation is followed by a linear time interpolation, it's also called the DFT-based channel estimators, which is use the time-domain transformation consisting of zero-padding to obtain the interpolation in frequency-domain[9].

### 2.2.2.3 Linear Interpolation (LI) Algorithm:

#### LI at PUSC allocation mode:

This algorithm first produces least squares estimates at the pilots and then uses them to linearly interpolate the channel in time and then in frequency. Given the PUSC tile shown in Figure 2.3.

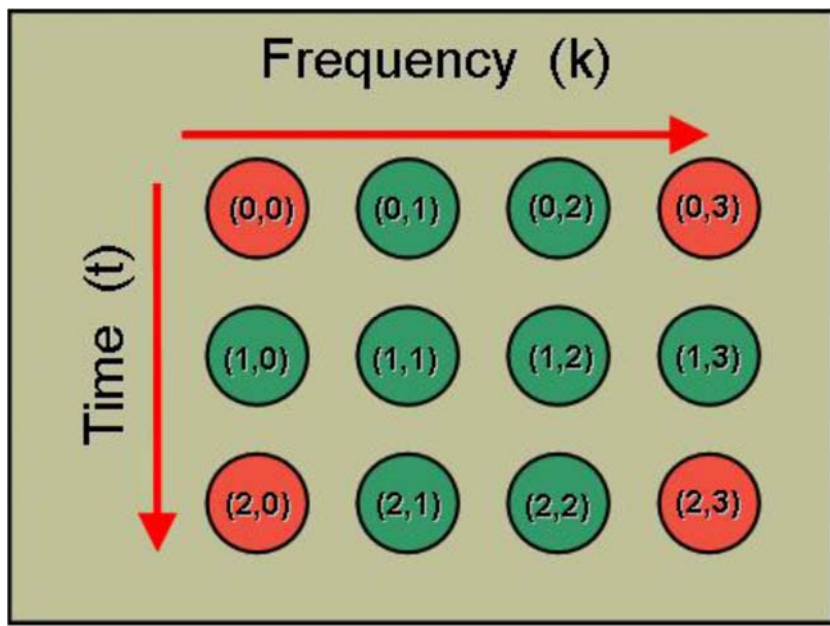


Figure 2.3 the PUSC tile

The contribution of noise depends on the signal to noise ratio. We see that the interpolation error equals zero if the channel is perfectly correlated within the PUSC tile. However, the delay spread is much longer and hence, the channel between the pilot subcarriers is less

correlated. This means the channel can change rapidly between adjacent subcarriers and introduce more interpolation error.

For SNR levels greater than 15dB, there is no improvement in the linear interpolation channel estimation performance and a system operating in this channel must choose a modulation code rate that can tolerate at least a MSE of -17dB. In addition, Doppler Spread does not affect channel estimation performances [2].

### **LI at AMC allocation mode:**

Linear interpolation is the channel estimation algorithm commonly employed right now. This algorithm estimates the channel at each pilot and then linearly interpolates the channels at the data subcarriers between two subcarriers and extrapolates the channel at the data subcarriers at the edges of the sub-channel. Given the arrangement shown in Figure 2.4.

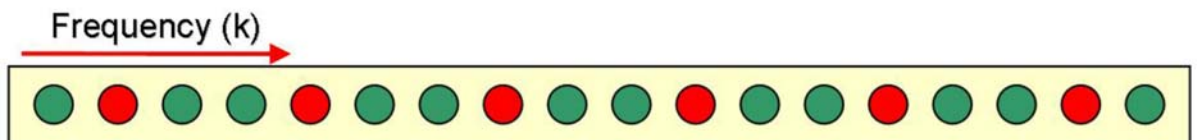


**Figure 2.4: Arrangement of Pilots in one OFDM symbol within one AMC**

Sub-channel under assumption that channel remains constant over 3 OFDM symbols to evaluate the linear interpolator. We derived the average MSE of an AMC sub-channel using the arrangement shown in

Figure 2.4. In this arrangement, there are 3 types of subcarriers: pilot subcarriers, interpolated subcarriers, and extrapolated subcarriers. To compute the average MSE in an AMC sub-channel, we derived the MSE for each type of subcarriers. The performance of the linear interpolation channel estimator depends on the interpolation error and noise.

The interpolation error term depends on the channel correlation and the noise term depends on the SNR of the channel. We can see that performance of the linear interpolator depends on the delay spread of the channel. However, we also observe that the performance of the linear interpolator in SUI-5 and Vehicular-B. In these channels, the frequency response changes too rapidly in frequency for the linear interpolator to accurately estimate the channel with the given pilot arrangement even as the SNR increases[2].

#### **2.2.2.4 Genie-Aided Channel Estimator:**

In PUSC channel estimation algorithms, we also use a genie-aided channel estimator to compare the performance of our channel estimators with one that has perfect channel knowledge. The idea to using the genie-aided estimator is to allow us to understand what the optimal channel estimation performance is in a WiMAX PUSC system. It can also be used to evaluate what performance a perfectly adaptive estimator could achieve.

To implement the genie-aided estimator, we took a copy of the transmitted symbol and copy of the received signal without any noise and correlated them together. These estimates were then passed to the



equalizer. A block diagram illustrating the implementation of the genie-aided channel estimator is shown in Figure 2.5[2].

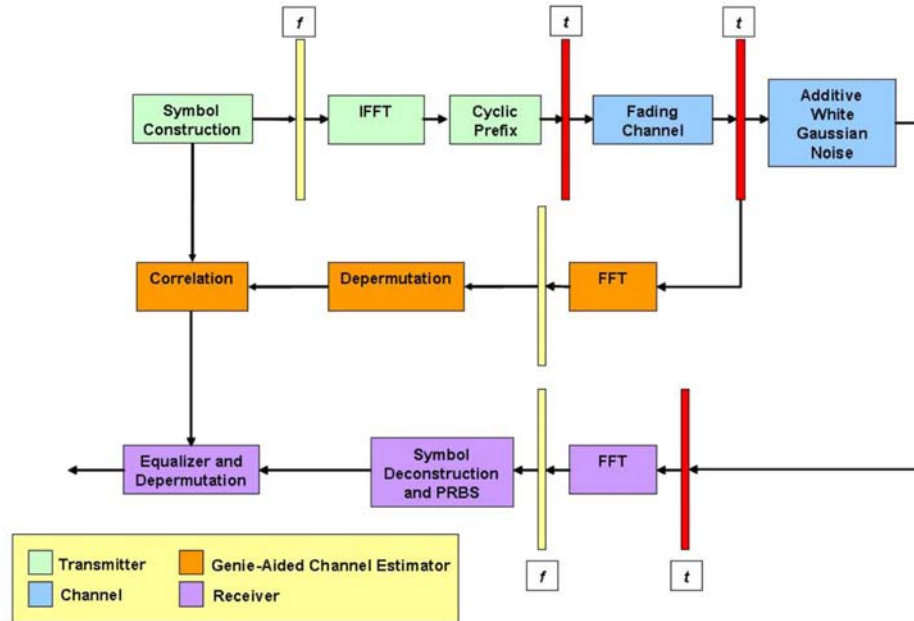


**Figure 2.5:Genie-aided Channel Estimator**

## **CHAPTER THREE**

### **CHANNEL ESTIMATION ALGORITHMS**

### **3.1 WiMAX Subcarrier Permutation Modes:**

In order to create the OFDM symbol in the frequency domain, the modulated symbols are mapped on to the subchannels that have been allocated for the transmission of the data block.

A subchannel, as defined in the IEEE 802.16e-2005 standard, is a logical collection of subcarriers. The number and exact distribution of the subcarriers that constitute a subchannel depend on the subcarrier permutation mode. The number of subchannels allocated for transmitting a data block depends on various parameters, such as the size of the data block, the modulation format, and the coding rate. In the time and frequency domains, the contiguous set of subchannels allocated to a single user or a group of users, in case of multicast—is referred to as the data region of the user(s) and is always transmitted using the same burst profile. In this context, a burst profile refers to the combination of the chosen modulation format, code rate, and type of FEC: convolution codes, turbo codes, and block codes.

It is important to realize that in WiMAX, the subcarriers that constitute a subchannel can either be adjacent to each other or distributed throughout the frequency band, depending on the subcarrier permutation mode. A distributed subcarrier permutation provides better frequency diversity, whereas an adjacent subcarrier distribution is more desirable for beam-forming and allows the system to exploit multiuser diversity[15].

Currently, Partial Usage of Subcarriers (PUSC) is the distributed subcarrier permutation and Adaptive Modulation and Coding (AMC) is

the adjacent subcarrier permutation WiMAX is required to support on the uplink.

The mobile WiMAX standard defines the following schemes as mandatory:

- PUSC, FUSC, and AMC for the downlink.
- PUSC and AMC for the uplink.

The interest here will be in uplink subcarrier permutation mode only.

### **3.1.1 Distributed Subcarrier Permutation (PUSC):**

For PUSC, the mapping of subcarriers to subchannels is different between the uplink and downlink.

In PUSC-UL, the first step is to remove logically null subcarriers; the remaining subcarriers are then mapped into tiles using PermBase-based permutation. Every 4 contiguous data subcarriers form a tile over 3 symbols. Pilots are allocated in each tile as shown in Figure 2.3. In each tile, one out of every three subcarriers is a pilot.

Tiles are mapped into slots, with 6 tiles per slot. The slots define the sub-channel index. The tile mapping to sub-channels is done using PermBase. Sub-channels are also formed by 6 tiles chosen according to a pre-defined permutation. Each tile has 4 pilots, so each sub-channel has 24 pilots and 48 data subcarriers. The high number of pilots provides a strong basis for data recovery[16].

### **3.1.2 Adjacent Subcarrier Permutation (AMC):**

In AMC, the permutation is the same for both the uplink and downlink. In this permutation, the first step is to remove logically null (guard) sub-carriers. Bins are then formed by creating groups of 9 contiguous subcarriers, the middle one being the pilot. Six bins are then joined to form a slot. This can be done in four different ways: 1 bin over 6 symbols, 2 bins over 3 symbols, 3 bins over 2 symbols or 6 bins over 1 symbol. Each of these ways is commonly represented as  $N \times M$ , where  $N$  is the number of bins and  $M$  is the number of symbols, for example, AMC  $2 \times 3$  stands for AMC with 2 bins over 3 symbols. The bins are mapped to sub-channels using the IDCell as the permutation base. Regardless of the  $N \times M$  combination used, the total number of data subcarriers per sub-channel is always 48.

AMC can be used both in the downstream and upstream. Its use of contiguous subcarriers makes this the only permutation scheme available for use with Advanced Antenna Systems (AAS)[16].

### **3.2 Channel Estimation Algorithms in PUSC:**

Partial Usage of Subcarriers (PUSC) is a one of two permutation modes that is used in WiMAX systems, which is classified as distributed permutation mode. At the PUSC mode the subcarriers are grouped into tiles, and to form subchannels it's pseudo-randomly allocated.

Each tile is consist of 12 received samples  $(t, k)$  for  $t = 0, \dots, 2$ , and  $k = 0, \dots, 3$  in which 4 are reserved for pilots. The set of pilot positions is  $P = \{(0,0), (0,3), (2,0), (2,3)\}$ . The channel estimation algorithm must

process each tile independently, because subchannels are composed of randomly selected tiles. That means no information from pilots in adjacent tiles can be used.

In each algorithm, the first step is to generate a baseline channel estimate at each received pilot.

Because both the transmitted and received signal are known at the receiver, we make estimates at the pilot subcarriers based on a least squares approach given by:

$$\hat{H}(t,k) = \frac{Y(t, k)}{X(t, k)} \text{ for } (t,k) \in P \quad (3.1)$$

The least squares estimate is the best estimate if there is no noise.

### 3.2.1 Linear Interpolation:

The linear interpolation algorithm is currently the common approach to channel estimation in PUSC. This algorithm first produces least squares estimates at the pilots and then uses them to linearly interpolate the channel in time and then frequency. Given the PUSC tile shown in Figure 2.3, the steps of the algorithm described mathematically are:

1. Perform Least Squares estimation at pilot positions using Equation 3.1.
2. Interpolate channel estimates in time at subcarrier between Pilots.

$$\hat{H}(1, 0) = \frac{1}{2}\hat{H}(0, 0) + \frac{1}{2}\hat{H}(2, 0) \quad (3.2)$$

$$\hat{H}(1, 3) = \frac{1}{2}\hat{H}(0, 3) + \frac{1}{2}\hat{H}(2, 3) \quad (3.3)$$

3. Interpolate Channel Estimates in Frequency at each OFDM symbol

$$\hat{H}(t, 1) = \frac{1}{3}\hat{H}(t, 0) + \frac{2}{3}\hat{H}(t, 3) \quad \text{for } t = 0, 2 \quad (3.4)$$

$$\hat{H}(t, 2) = \frac{1}{3}\hat{H}(t, 0) + \frac{2}{3}\hat{H}(t, 3) \quad \text{for } t = 0, 2 \quad (3.5)$$

### **Performance Analysis for Linear Interpolation:**

Now consider the mean-squared error (MSE) performance of the linear interpolator in the PUSC tile. To evaluate its performance, the calculation of the MSE at each data subcarrier and average them over the 8 data subcarriers in the PUSC tile, must be done. In the PUSC tile, there are 3 types of subcarriers when using the linear interpolator. The first are the subcarriers that are interpolated in time from step 2 of the estimation process. These subcarriers can be defined as  $A = \{(1, 0), (1, 3)\}$ .

The second are the subcarriers interpolated in frequency in OFDM symbols containing pilots. Because there are two subcarriers in the same OFDM symbol in which the channel estimate is produced by interpolating the pilots in frequency, must calculate the arithmetic average MSE over the pair of subcarriers. We define these subcarrier

positions to be  $B = \{B1, B2\}$ , where  $B1 = \{(0, 1), (0, 2)\}$  and  $B2 = \{(2, 1), (2, 2)\}$ . This simplifies calculations since the average MSE of the subcarriers in  $B1$  and  $B2$  are the same. The third are the subcarriers in the middle which are interpolated in both time and frequency. And these subcarrier positions is defined as  $C = \{(1, 1), (1, 2)\}$ .

In the calculation of average MSE, it's assumed that each channel estimate was made according to Equation 3.1, Equation 3.2, Equation 3.3, Equation 3.4, and Equation 3.5.

If also assume that for the pilot constellation points all have the same magnitude,  $|X(t, k)| = A$  for  $(t, k) \in P$ , then the mean-squared error derivation for each type of subcarrier is:

1. Mean-squared error at  $(t, k) \in A$  :

$$\begin{aligned} \text{MSE}_A &= E[|\hat{H}(t, k) - H(t, k)|^2] \\ &= \sigma^2_H \left\{ \frac{2}{3} \text{Rt}[0] + \frac{1}{4} (\text{Rt}[2] - \text{Rt}[-2] - \text{Rt}[1] \right. \\ &\left. + \text{Rt}[-1]) \right\} + \frac{1}{2} \frac{\sigma_v^2}{A^2} \end{aligned} \quad (3.6)$$

Where  $\text{Rt}[\Delta t]$  is the time-domain correlation function

2. Average mean-squared error for  $\{(t, k), (t, k+1)\} \in B_t$  for  $t = \{0, 2\}$ .

$$\begin{aligned} \text{MSE}_{B_t} &= \frac{1}{2} [\text{MSE}(t, k) + \text{MSE}(t, k+1)] \\ &= \frac{1}{2} \sum_{l=1}^2 E[|\hat{H}(t, l) - H(t, l)|^2] \end{aligned}$$



$$\begin{aligned}
&= \sigma^2_H \left\{ \frac{14}{9} \text{Rf}[0] + \frac{2}{9} (\text{Rf}[3] + \text{Rf}[-3]) - \frac{4}{3} (\text{Rf}[1] + \text{Rf}[-1]) \right. \\
&\left. - \frac{2}{3} (\text{Rf}[2] + \text{Rf}[-2]) \right\} + \frac{5 \sigma_v^2}{9 A^2} \tag{3.7}
\end{aligned}$$

Where  $\text{Rf} [\Delta k]$  is the frequency-domain correlation function.

3. Mean-squared error at  $(t,k) \in C$  :

$$\begin{aligned}
\text{MSE}_C &= E[|\hat{H}(t, k) - H(t, k)|^2] \\
&= \frac{23}{18} \text{RH} [0, 0] + \frac{5}{36} (\text{RH} [2, 0] + \text{RH} [-2, 0]) + \frac{1}{9} (\text{RH} [0, 3] \\
&+ \text{RH} [0, -3]) + \frac{1}{18} (\text{RH} [2, 3] + \text{RH} [-2, 3]) + \frac{1}{9} (\text{RH} [2, -3] \\
&+ \text{RH} [-2, -3]) - \frac{1}{3} (\text{RH} [1, 1] + \text{RH} [1, -1]) + \frac{1}{9} (\text{RH} [-1, 1] \\
&+ \text{RH} [-1, -1]) - \frac{1}{6} (\text{RH} [1, 2] + \text{RH} [1, -2]) + \frac{1}{9} (\text{RH} [-1, 2] \\
&+ \text{RH} [-1, -2]) + \frac{5 \sigma_v^2}{18 A^2} \tag{3.8}
\end{aligned}$$

Where  $\text{RH}[\Delta t, \Delta k]$  is the channel autocorrelation function for the frequency response at different times and frequencies.

The average MSE in a PUSC tile is:

$$\text{MSE}_{\text{LI-PUSC}} = \frac{2}{8} \text{MSE}_A + \frac{4}{8} \text{MSE}_B + \frac{2}{8} \text{MSE}_C \tag{3.9}$$

From the above theoretical calculations the average MSE depends on two factors: interpolation error and noise.

The interpolation error depends on the correlation of the channel. Interpolation error occurs because the estimator uses a first-order approximation of the channel when the channel may be nonlinear at the data subcarriers between the pilots.

The contribution of noise depends on the signal to noise ratio.

### 3.2.2 4-Pilot Averaging:

Another approach to performing channel estimation within a PUSC tile is averaging the 4 received pilots and using that result to estimate the channel. The motivation to this method is that in channels where noise is the dominant contributor to distortion, the channel estimates at the pilot positions are too corrupted to use for interpolation. So the idea behind this technique is that a better estimate of the channel could be made by using all the pilots to average out some of the noise and using this estimate at all data subcarriers in the tile. The steps of this algorithm mathematically are given by:

1. Perform Channel Estimation at pilot positions using Equation 3.1.
2. Average the 4 channel estimates at the pilot subcarriers and use at each data subcarrier. The set of data subcarriers within a tile is

$$D = \{(0, 1), (0, 2), (1, 0), (1, 1), (1, 2), (1, 3), (2, 1), (2, 2)\}$$

$$\hat{H}(t, k) = \frac{1}{4}\hat{H}(0, 0) + \frac{1}{4}\hat{H}(2, 0) + \frac{1}{4}\hat{H}(0, 3) + \frac{1}{4}\hat{H}(2, 3) \quad (3.10)$$

## Performance Analysis for 4-Pilot Averaging:

Similar to the analytical model for the linear interpolator, analytical model has created to evaluate the channel estimation performance with the 4-pilot averaging technique. If the channel estimate calculated using Equation 3.10, then the MSE at each subcarrier using the 4-pilot averaging technique is given by:

$$\begin{aligned}
 \text{MSE}_D(t, k) &= E[|\hat{H}(t, k) - H(t, k)|^2] \\
 &= \frac{5}{4} \text{RH}[0, 0] + \frac{1}{8} (\text{RH}[2, 0] + \text{RH}[-2, 0]) + \frac{1}{8} (\text{RH}[0, 3] \\
 &\quad + \text{RH}[0, -3]) \\
 &\quad + \frac{1}{16} (\text{RH}[2, 3] + \text{RH}[-2, 3] + \text{RH}[2, -3] + \text{RH}[-2, -3]) \\
 &\quad - \frac{1}{4} (\text{RH}[t, k] + \text{RH}[-t, -k]) - \frac{1}{4} (\text{RH}[t-2, k] + \text{RH}[2-t, -k]) \\
 &\quad - \frac{1}{4} (\text{RH}[t, k-3] + \text{RH}[-t, 3-k]) \\
 &\quad - \frac{1}{4} (\text{RH}[t-2, k-3] + \text{RH}[2-t, 3-k]) + \frac{1}{4} \frac{\sigma_v^2}{A^2} \tag{3.11}
 \end{aligned}$$

The average MSE within the PUSC tile using the 4-pilot averaging method is given by:

$$\begin{aligned}
 \text{MSE}_{4\text{avg}} &= \frac{1}{8} \left\{ \sum_{k=1}^2 \text{MSE}_D(0, k) + \sum_{k=0}^3 \text{MSE}_D(1, k) \right. \\
 &\quad \left. + \sum_{k=1}^2 \text{MSE}_D(2, k) \right\} + \frac{1}{4} \frac{\sigma_v^2}{A^2} \tag{3.12}
 \end{aligned}$$

Again, we see that the 4-pilot averaging channel estimation performance depends on the interpolation error and noise.

In essence, the 4-pilot averaging algorithm estimates the channel with a constant. Therefore, inherent in the 4-pilot averaging technique is the assumption that the channel is highly correlated. However, this estimator to degrade rapidly as the channel becomes less correlated within the tile due to increased delay spread and/or Doppler spread.

### **3.3 Channel Estimation Algorithms in AMC:**

Adaptive Modulation and Coding (AMC) is another permutation supported by WiMAX. AMC is classified as an adjacent subcarrier permutation in which subchannels are composed of adjacent subcarriers and allocated to users by the MAC scheduler based on their unique channel conditions. Each subchannel is composed of 18 adjacent subcarriers over 3 OFDM symbols with 6 pilot subcarriers per subchannel.

Consider the scenario when two adjacent subchannels (36 adjacent subcarriers over 3 OFDM symbols) are allocated to a user in which pilots from both subchannels can be used to aid in channel estimation. Similar to the analysis performed for PUSC.

To simplify the channel estimation problem, assume that the channel remains constant over 3 OFDM symbols. This assumption allows us to assume that the channel estimate at a particular subcarrier can be used to estimate the same subcarrier at a different time within the subchannel.

By simplifying the problem in this manner, it can be apply channel estimation algorithms that process one OFDM symbol with  $M = 18, 36$  adjacent subcarriers and a pilot every 3 subcarriers and 1 data subcarrier at the edge of each subchannel. Figure 2.4 shows the arrangement of pilots within one OFDM symbol under this assumption.

The first step is to generate baseline channel estimates at the pilot subcarriers using the least squares estimate. Using the arrangement shown in Figure 2.4, if let  $P$  be the total number of pilots for  $M$  total number of subcarriers, then there is a pilot every  $D = M/P$  subcarriers.

For AMC,  $D=3$ . Therefore, the estimate of the channel at the pilot subcarriers is given by:

$$\hat{H}(t, 3p+1) = \frac{Y(t, 3p+1)}{X(t, 3p+1)} \quad \text{for } p = 0, 1, \dots, P-1 \quad (3.13)$$

### 3.3.1 Linear Interpolation:

Linear interpolation is the channel estimation algorithm commonly employed right now. This algorithm estimates the channel at each pilot and then linearly interpolates the channels at the data subcarriers between two subcarriers and extrapolates the channel at the data subcarriers at the edges of the subchannel. Given the arrangement shown in Figure 2.4, the steps of the algorithm described mathematically are

1. Generate Baseline Channel Estimates at Pilot Positions using Equation 3.13.
2. Interpolate Channel Estimates in Frequency at Subcarrier between Pilots:

$$\hat{H}(t, 3p+2) = \frac{2}{3}\hat{H}(t, 3p+1) + \frac{1}{3}\hat{H}(t, 3p+4) \quad \text{for } p = 0, 1, \dots, P-1 \quad (3.14)$$

$$\hat{H}(t, 3p + 3) = \frac{1}{3}\hat{H}(t, 3p + 1) + \frac{2}{3}\hat{H}(t, 3p + 4) \quad \text{for } p = 0, 1, \dots, P-1 \quad (3.15)$$

3. Extrapolate Channel Estimates in Frequency at Subcarriers at Edges of Subchannel:

$$\hat{H}(t, 0) = \frac{2}{3}\hat{H}(t, 1) + \frac{1}{3}\hat{H}(t, 4) \quad (3.16)$$

$$\hat{H}(t, M-1) = \frac{1}{3}\hat{H}(t, M-2) + \frac{2}{3}\hat{H}(t, M-5) \quad (3.17)$$

### **Performance Analysis for Linear Interpolation:**

To evaluate the linear interpolator, it can be derived the average MSE of an AMC subchannel using the arrangement shown in Figure 2.4. In this arrangement, there are 3 types of subcarriers: pilot subcarriers, interpolated subcarriers, and extrapolated subcarriers. To compute the average MSE in an AMC subchannel, it must derive the MSE for each type of subcarriers. The derivations below are provided by [2].

In the derivation, if assume that the pilot constellation points all have the same magnitude,  $|X(t, 3p+1)| = A$  for  $p=0,1,\dots,P-1$ , then the MSE at each type of subcarrier is given by

1. MSE at pilot subcarriers from Step 1

$$\mathbf{MSE}_P = E\{\|\hat{H}(t, 3p+1) - H(t, 3p+1)\|^2\}$$

$$= \frac{\sigma_v^2}{A^2} \quad (3.18)$$

2. Arithmetic average MSE over interpolated subcarriers from Step 2

$$\begin{aligned} \mathbf{MSE}_I &= \frac{1}{2} \sum_{l=1}^2 E\{\|\hat{H}(t, 3p+1+l) - H(t, 3p+1+l)\|^2\} \\ &= \sigma_H^2 \left\{ \frac{14}{9} R_f[0] + \frac{2}{9} (R_f[3] + R_f[-3]) - \frac{4}{3} (R_f[1] + R_f[-1]) - \right. \\ &\quad \left. \frac{2}{3} (R_f[2] + R_f[-2]) \right\} + \frac{5\sigma_v^2}{9A^2} \end{aligned} \quad (3.19)$$

3. MSE at extrapolated subcarriers from Step 3

$$\begin{aligned} \mathbf{MSE}_E &= E\{\|\hat{H}(t, 0) - H(t, 0)\|^2\} \\ &= E\{\|\hat{H}(t, M-1) - H(t, M-1)\|^2\} \\ &= \sigma_H^2 \left\{ \frac{26}{9} R_f[0] + \frac{1}{3} (R_f[4] + R_f[-4]) \right. \\ &\quad \left. - \frac{4}{3} (R_f[1] + R_f[-1]) - \frac{4}{9} (R_f[3] + R_f[-3]) \right\} \\ &\quad + \frac{17\sigma_v^2}{9A^2} \end{aligned} \quad (3.20)$$

Given the MSE at the pilot, interpolated, and extrapolated subcarriers, it's easy to calculate the average MSE over an AMC subchannel with M adjacent subcarriers and P pilot subcarriers.

$$\mathbf{MSE}_{LI-AMC} = \frac{1}{M} [P \cdot \mathbf{MSE}_P + (M - P - 2) \cdot \mathbf{MSE}_I + 2 \cdot \mathbf{MSE}_E] \quad (3.21)$$

From the derivation above, the performance of the linear interpolation channel estimator depends on the interpolation error and noise. The interpolation error term depends on the channel correlation and the noise term depends on the SNR of the channel. Using the derivation,

Again we see that performance of the linear interpolator depends on the delay spread of the channel.

### **3.3.2 Frequency Smoothing:**

In this algorithm, the idea is to smooth the frequency-domain channel estimates at the pilots by applying a rectangular window in the time-domain. Because of the duality between the time and frequency domain, this method is analogous to applying a low-pass filter in the time-domain (or convolution with a sinc function in the frequency-domain). However, because in AMC there are only pilots every  $D = 3$  subcarriers, 3 images of the channel impulse response will appear in the time domain. Because of these images, the window size must be selected such that the images are eliminated.

A block diagram illustrating the system implementing the frequency smoothing algorithm is shown in Figure 3.1.



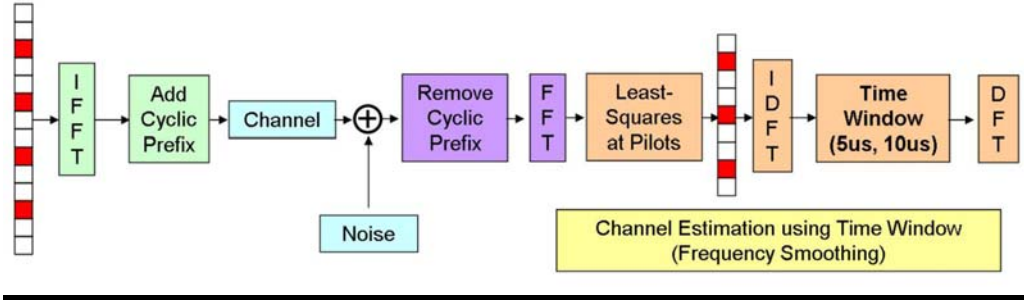


**Figure 3.1: Block Diagram of WiMAX with Frequency Smoothing Channel Estimation Algorithm.**

If assume that each pilot has the same magnitude,  $|X(t, 3p + 1)| = A$  for  $p = 0, 1, \dots, P-1$ , then the steps of the algorithm described mathematically can be described as:

1. Generate Baseline Channel Estimates at Pilot Positions using Equation 3.11.
2. Construct vector of length  $M$  with baseline channel estimates at pilot subcarriers and zero at the data subcarrier positions. Use  $M$ -point IDFT to transform baseline channel estimate to time domain.

$$\hat{h}[m] = IDFT\{\hat{H}\} = h[m] + \frac{v[m]}{A} \quad (3.22)$$

3. Zero out samples beyond a set time threshold or multiply time domain response by a rectangular window  $w[m]$  of length  $L$  equal to time threshold. To calculate  $L$ , we select a desired window size in time and use the formula below to calculate the number of samples that it corresponds to:

$$L = \text{round}\left(M \cdot \frac{\text{WindowSizeInTime}}{\text{SymboleDuration}}\right) \quad (3.23)$$

$$w[m] = \begin{cases} 1 & \text{form } = 0, 1, \dots, L - 1 \\ 0 & \text{form } = L, L + 1, \dots, M - 1 \end{cases} \quad (3.24)$$

$$\hat{h}_{fs}[m] = w[m]\hat{h}[m] \quad (3.25)$$

4. Transform windowed response back to the frequency domain using M-point DFT to obtain channel estimates

$$\hat{H}_{fs}(k) = \sum_{m=0}^{L-1} \hat{h}_{fs}[m] e^{-j2\pi k \frac{m}{M}} + \sum_{m=0}^{L-1} \frac{v[m]}{A} e^{-j2\pi k \frac{m}{M}} \quad (3.26)$$

In general, choosing a window size that corresponds exactly to the maximum delay spread of the channel is much appropriate. Assuming that the delay spread of the channel is less than 1/3 the symbol duration, this would allow to reject the images and the most noise possible without losing any channel energy and inducing a bias in our channel estimates. However, the delay spread is typically unknown so a fixed window size is pre-determined. But if choosing an arbitrary window length, L, such that it is longer than the channel delay spread and eliminates the images, then using Equation 3.22, the average MSE at each subcarrier within the AMC subchannel is given by

$$\begin{aligned} \text{MSE}_{FS} &= E \left\{ \left\| \hat{H}_{fs}(t, k) - H(t, k) \right\|^2 \right\} \text{ for } k = 0, 1, \dots, M - 1 \\ &= \frac{L}{M} \frac{\sigma_v^2}{A^2} \end{aligned} \quad (3.27)$$

From Equation 3.23, the frequency smoothing channel estimation performance depends only on noise if choosing  $L$  to be longer than the length of the channel impulse response. The frequency smoothing channel estimator reduces the effect of noise by a factor of  $L/M$ .

And when compare the frequency smoothing performance to the linear interpolation performance, it can be seen that even in a channel that was perfectly correlated, the performance of the frequency smoothing algorithm will be better as long as  $L$  is chosen to be less than  $\frac{4P+5M+24}{9}$ .

In AMC ( $P = 6$ ,  $M = 18$ ), if choose  $L < 15$ , then the frequency smoothing estimator will outperform the linear interpolator. In WiMAX, for  $N = 1024$  and cyclic prefix fraction =  $1/8$ , the symbol duration is  $102.9\mu\text{s}$  so  $L = 15$  corresponds to window length of  $85.75\mu\text{s}$ . Typically, the channel delay spread will be less than  $10\mu\text{s}$  and out of all the channels that had been tested before. Therefore, for most channels, it can select a window length such that, it will outperform the linear interpolator.

**CHAPTER FOUR**  
**SIMULATION**

## 4.1 PUSC channel Estimation Simulation:

In the simulations, the objective is to first evaluate the performance of the linear interpolation channel estimation algorithm in different types of channel conditions and compare it to the 4-pilot averaging channel estimator. We used the results to identify conditions where improving the channel estimator was warranted.

Of most interest here are relationships between the signal bandwidth and the channel coherence bandwidth, and between the slot time duration and the channel coherence time.

### 4.1.1 Simulation Parameters:

In a WiMAX system operated at a typical bandwidth  $BW=10\text{MHz}$ , the subcarrier spacing:

$$\Delta f = \text{floor}(n \cdot BW / 8000) * 8000 / K, \quad (4.1)$$

Where  $n$  is the sampling factor with a typical value of  $(8/7)$ ,  $K=2048$  is the number of IFFT/ FFT points, and  $\text{floor}(x) = \lfloor x \rfloor$  is the largest integer not greater than  $x$ .

The result is  $\Delta f \approx 5.58\text{kHz}$ , which is relatively narrow compared to typical channel coherence bandwidths, because a typical value of coherence bandwidth is in the range of 50kHz to 500kHz for many cellular systems in urban areas, and in the range of 1MHz to 3MHz for many radio channels in indoor environments. Thus, the correlations among the four neighbouring frequency subcarriers inside a tile will be

sufficiently high, and the averaging algorithm is appropriate in the frequency dimension.

### **The Modulation Scheme:**

The WiMAX profile also specifies many modulation and code rates to allow the system more control of the data rates. On the downlink, QPSK, 16-QAM, and 64-QAM are the required modulations. On the uplink, QPSK and 16-QAM are the required modulations while 64-QAM is optional. In this simulation 16-QAM modulation scheme will be used.

### **Channel Impulse Response Model:**

To model the multipath fading channel, the channel is represented as a time-varying impulse response.

$$h(t, \tau) = \sum_{i=1}^P \alpha_i(t) \cdot \delta(\tau - \tau_i) \quad (4.2)$$

Where  $\alpha_i(t)$  is the complex tap gain and assumed to be a complex Gaussian randomvariable,  $\tau_i$  is the delay of the  $i^{th}$  path, and P is the number of paths in the channel profile. Then, by definition, the channel frequency response is defined as:

$$H(t, f) = \sum_{i=1}^P \alpha_i(t) \cdot e^{-i2\pi f\tau_i} \quad (4.3)$$

### 4.1.2 Linear Interpolation vs. 4-Pilot Averaging:

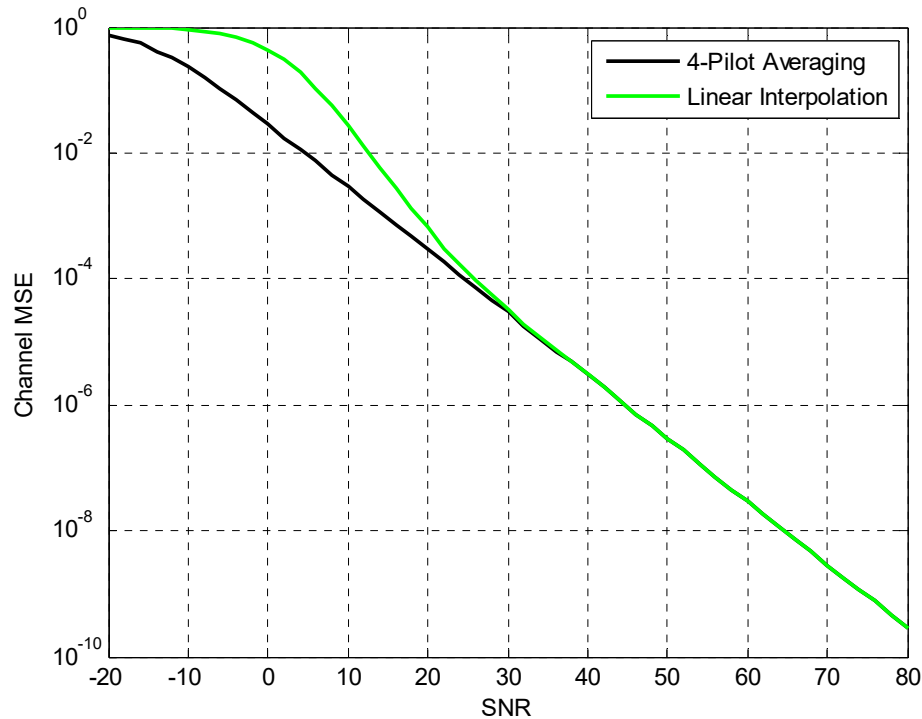


**Figure 4.1:** Comparison between Linear Interpolation and 4-Pilot

Averaging in term of MSE

From these plots, we can conclude that the 4-pilot averaging method does perform better than the linear interpolator at low SNR. We can explain this result by the fact that at low SNR, noise is the dominant contributor to distortion and the 4-pilot averaging method reduces about 3dB more noise than the linear interpolator.

However, as we increase the SNR, we can see that the relative performance of the 4-pilot averaging estimator to the linear interpolator decreases to be as equal as linear interpolation.

## **4.2 AMC channel Estimation Simulation:**

### **4.2.1 Simulation Parameter:**

For this experiment, we chose to test the performance of the linear interpolator and frequency smoothing algorithm for AMC subchannel sizes of  $M = 18$  and  $M = 36$  and assuming a pilot arrangement as shown in Figure 2.4. For the frequency smoothing algorithm, we chose to test time window lengths of  $5\mu\text{s}$ . The  $5\mu\text{s}$  window was chosen because in general, many of the channels encountered in practice have a maximum delay spread less than  $5\mu\text{s}$ .

### **4.2.2 Linear Interpolation vs. Frequency Smoothing:**

From figure 4.2, we observe that the frequency smoothing algorithm is generally better than the linear interpolator. In the low delay spread channels we expect the frequency smoothing algorithm to always be better because it rejects more noise than the linear interpolator. However, for the higher delay spread channels we see that the performance of the frequency smoothing algorithm will floor at some point and that the linear interpolator will outperform the frequency smoothing estimator beyond a certain SNR point. We can attribute this flooring to the frequency smoothing algorithm not using a window size large enough to capture all the channel's energy.



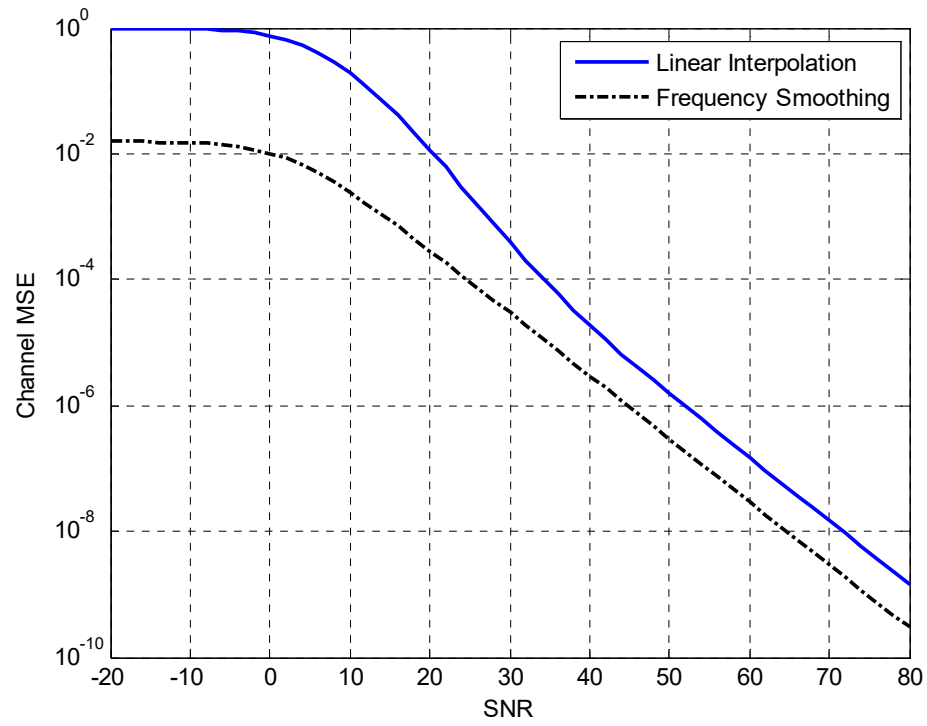


**Figure 4.2:** Comparison between Linear Interpolation and Frequency Smoothing in term of MSE

## **CHAPTER FIVE**

### **CONCLUSION**

## **5.1 CONCLUSION:**

In our study, we explored many channel estimation algorithms that can be used in WiMAX. Channel estimation is an important feature in any wireless communication system because it aids the receiver in undoing any distortion in the transmitted signal caused by the wireless channel. If the channel estimator has good tracking capabilities, it can significantly improve the coverage, throughput, and reliability of the overall system.

WiMAX utilizes pilots to aid in channel estimation and arranges the pilots differently depending on the permutation it employs. In PUSC, we analyzed the performance of the linear interpolator and 4-pilot averaging and observed that the 4-pilot averaging performed better in low SNR channels. But as the SNR increased and the channel delay spread and Doppler spread increased, we observed that the linear interpolator performed better. In AMC, we introduced a frequency smoothing algorithm and compared its performance to the linear interpolator. We observed that the frequency smoothing algorithm generally outperformed the linear interpolator except when the window length was not chosen long enough to capture all of the channel's energy.

## **5.2 Future Work:**

While this thesis covers much in the area of channel estimation for WiMAX there are still some areas in which this study can be expanded upon.

1. Study of the time evolution of the channel - In this study, our focus was primarily on channel estimation and interpolation in

frequency. This study could be expanded to include an analysis about the evolution of the channel in time and algorithms that can be applied across the time.

2. Development of a link-level simulator supporting AMC and -in our study for AMC, we used MSE as our primary metric to evaluate each algorithm. However, a better metric to evaluate each algorithm is bit-error rate, frame-error rate, and throughput and to accomplish this, we need to integrate our algorithm with a link-level simulator with all the components in a WiMAX system.

## References:

- [1] S. Ahmadi, *Mobile WiMAX: A systems approach to understanding IEEE 802.16 m radio access technology*: Academic Press, 2010.
- [2] K. Ho and A. Kwasinski, "Uplink channel estimation in WiMAX," in *2009 IEEE Wireless Communications and Networking Conference*, 2009, pp. 1-6.
- [3] F. Ohrtman, "WiMAX handbook," ed: McGraw-Hill, 2005.
- [4] P. K. Pradhan, S. K. Patra, O. Faust, and B. K. Chua, "Channel estimation algorithms for OFDM systems," *International Journal of Signal and Imaging Systems Engineering*, vol. 5, pp. 267-273, 2012.
- [5] H. Arslan, "Channel estimation for wireless OFDM systems," *IEEE Surveys and Tutorials*, vol. 9, pp. 18-48, 2007.
- [6] C. R. Athaudage and A. D. S. Jayalath, "Enhanced MMSE channel estimation using timing error statistics for wireless OFDM systems," *IEEE Transactions on Broadcasting*, vol. 50, pp. 369-376, 2004.
- [7] J. Hwang, "Simplified Channel Estimation Techniques for OFDM Systems with Realistic Indoor Fading Channels," 2009.
- [8] M. Singh, M. Singh, and A. Goraya, "Block based Channel Estimation Algorithms for OFDM-IEEE 802.16 e (Mobile

WiMAX) System," *International Journal of Computer Applications*, vol. 13, pp. 0975-8887, 2011.

- [9] Y. Shen, P. C. Cosman, L. B. Milstein, and E. F. Martinez, "On Uplink Channel Estimation in WiMAX Systems," *Advancing the Next-Generation of Mobile Computing: Emerging Technologies: Emerging Technologies*, p. 103, 2012.
- [10] H. Hoang-Ngoc, Q. Nguyen-Duc, and L. Pham-Hong, "An advanced pilot arrangement combined with channel estimation based on enhanced MMSE algorithm for mobile WiMAX," in *Control, Automation and Information Sciences (ICCAIS), 2012 International Conference on*, 2012, pp. 197-201.
- [11] H. Shatila, M. Khedr, and J. H. Reed, "Channel estimation for WiMaX systems using fuzzy logic cognitive radio," in *2009 IFIP International Conference on Wireless and Optical Communications Networks*, 2009, pp. 1-6.
- [12] Q. N. Duc, L. P. Hong, and T. L. Thanh, "An enhanced algorithm of channel estimation based on extended Kalman Filter for mobile WiMAX," in *Control, Automation and Information Sciences (ICCAIS), 2012 International Conference on*, 2012, pp. 132-136.
- [13] Y. Wang, "Study of Interpolation Algorithm for WIMAX-OFDM System," *Journal of Information & Computational Science*, vol. 9, pp. 3673-3681, 2012.
- [14] K. Li, X. Song, M. O. Ahmad, and M. Swamy, "An improved multicell MMSE channel estimation in a massive MIMO system,"

*International Journal of Antennas and Propagation*, vol. 2014, 2014.

- [15] J. G. Andrews, A. Ghosh, and R. Muhamed, *Fundamentals of WiMAX: understanding broadband wireless networking*: Pearson Education, 2007.
  
- [16] L. Korowajczuk, *LTE, WiMAX and WLAN network design, optimization and performance analysis*: John Wiley & Sons, 2011.
  
- [17] (2016).Available  
[http://en.pudn.com/search\\_db.asp?keyword=wimax+matlab](http://en.pudn.com/search_db.asp?keyword=wimax+matlab)
  
- [18] (2016).Available <http://www.edaboard.com/thread71584.html>
  
- [19] (2016).Available  
<https://www.mathworks.com/help/lte/ug/channel-estimation.html>
  
- [20]  
(2016).Available[https://en.wikipedia.org/wiki/Coherence\\_bandwidth](https://en.wikipedia.org/wiki/Coherence_bandwidth)
  
- [21] (2016).Available  
<http://www.wirelesscommunication.nl/reference/chaptr03/cohbw/cohbw.htm>

## Appendix A:

```
clc, clear, close all
snr_dB = [0:2:40]; % SNR in dB
snr_lin = 10.^(snr_dB/10); % SNR linear
sigma2_n = 1./snr_lin; % Variance of additive white
Gaussian
Nch = 4; % Number of taps within the tile
pilot_qpsk=3;
pilot_qam=13;
carrier_spacing=11.16*10^3 %subcarriere spacing in WiMAX
J0=1;
% generation of data
user_data=boolean(randint(1,32,2));
for t=1:2:numel(user_data)
qpsk_inputs((t+1)/2)=bi2de([user_data(t+1) user_data(t)]);
end
for t=1:4:numel(user_data)
qam_inputs((t+3)/4)=bi2de([user_data(t+3) user_data(t+2)
user_data(t+1) user_data(t)]);
end

% adding pilot signal
piloted_qpsk_data=[]
for t=1:8:numel(qpsk_inputs)
piloted_qpsk_data=[piloted_qpsk_data;pilot_qpskqpsk_inputs(t)
qpsk_inputs(t+1) pilot_qpsk;qpsk_inputs(t+2) qpsk_inputs(t+3)
qpsk_inputs(t+4) qpsk_inputs(t+5);pilot_qpskqpsk_inputs(t+6)
qpsk_inputs(t+7) pilot_qpsk];
end
piloted_qam_data=[]
for t=1:8:numel(qam_inputs)
piloted_qam_data=[piloted_qam_data;pilot_qamqam_inputs(t)
qam_inputs(t+1) pilot_qam;qam_inputs(t+2) qam_inputs(t+3)
qam_inputs(t+4) qam_inputs(t+5);pilot_qamqam_inputs(t+6)
qam_inputs(t+7) pilot_qam];
end
qam_mod=qammod(piloted_qam_data,16)
ofdm_s=ifft(qam_mod)
```



```

%the receiver

%demodulation
ofdm_d=fft(ofdm_s)
qam_demod=qamdemod(ofdm_d,16)

%pilot extraction
unpiloted_qam_data=[]
received_data=[]
for t=1:12:numel(qam_demod)
unpiloted_qam_data=[unpiloted_qam_dataqam_demod(t+1) qam_demod(t+2)
qam_demod(t+4) qam_demod(t+5) qam_demod(t+6) qam_demod(t+7)
qam_demod(t+9) qam_demod(t+10) ]
end
for t=1:numel(unpiloted_qam_data)
received_data=[received_datafliplr(de2bi(unpiloted_qam_data(t),4))]
end

nCP = 8;%round(Tcp/Ts);
nFFT = 64;
NT = nFFT + nCP;
F = dftmtx(nFFT)/sqrt(nFFT);

MC = 1500;

EbNodB = -20:2:80;
snr = 10.^(EbNodB/10);
beta = 17/9;
M = 16;
modObj = modem.qammod(M);
demodObj = modem.qamdemod(M);
L = 5;
ChEstLI = zeros(1,length(EbNodB));
ChEst4PA = zeros(1,length(EbNodB));
TD_ChEstLI = zeros(1,length(EbNodB));

```

```

TDD_ChEstALI = zeros(1,length(EbNodB));
TDQabs_ChEstLI = zeros(1,length(EbNodB));

for ii = 1:length(EbNodB)
disp('EsN0dB is '); disp(EbNodB(ii));tic;
ChMSE_LS = 0;
ChMSE_LMMSE=0;
    TDMSE_LMMSE =0;
    TDDMSE_LMMSE=0;
TDQabsMSE_LMMSE =0;
for mc = 1:MC
% Random channel taps
    g = randn(L,1)+li*randn(L,1);
    g = g/norm(g);
    H = fft(g,nFFT);
% generation of symbol
    X = randi([0 M-1],nFFT,1); %BPSK symbols
    XD = modulate(modObj,X)/sqrt(10); % normalizing symbol power
    x = F'*XD;
xout = [x(nFFT-nCP+1:nFFT);x];
% channel convolution and AWGN
    y = conv(xout,g);
nt =randn(nFFT+nCP+L-1,1) + li*randn(nFFT+nCP+L-1,1);
    No = 10^(-EbNodB(ii)/10);
    y = y + sqrt(No/2)*nt;
% Receiver processing
    y = y(nCP+1:NT);
    Y = F*y;

HhatLS = Y./XD;
ChMSE_LS = ChMSE_LS + ((H -HhatLS)'*(H-HhatLS))/nFFT;

Rhh = H*H';
    W = Rhh/(Rhh+(beta/snr(ii))*eye(nFFT));
HhatLMMSE = W*HhatLS;
ChMSE_LMMSE = ChMSE_LMMSE + ((H -HhatLMMSE)'*(H-HhatLMMSE))/nFFT;

ghatLS = ifft(HhatLS,nFFT);
Rgg = g*g';
    WW = Rgg/(Rgg+(beta/snr(ii))*eye(L));

```

```

ghat = WW*ghatLS(1:L);
TD_HhatLMMSE = fft(ghat,nFFT);%
    TDMSE_LMMSE = TDMSE_LMMSE + ((H -TD_HhatLMMSE)'*(H-
TD_HhatLMMSE))/nFFT;

ghatLS = ifft(HhatLS,nFFT);
Rgg = diag(g.*conj(g));
    WW = Rgg/(Rgg+(beta/snr(ii))*eye(L));
ghat = WW*ghatLS(1:L);
TDD_HhatLMMSE = fft(ghat,nFFT);%
    TDDMSE_LMMSE = TDDMSE_LMMSE + ((H -TDD_HhatLMMSE)'*(H-
TDD_HhatLMMSE))/nFFT;

ghatLS = ifft(HhatLS,nFFT);
TDQabs_HhatLMMSE = fft(ghat,nFFT);%
TDQabsMSE_LMMSE = TDQabsMSE_LMMSE + ((H -TDQabs_HhatLMMSE)'*(H-
TDQabs_HhatLMMSE))/nFFT;

end

ChEstLI(ii) = ChMSE_LS/MC;
ChEst4PA(ii)=ChMSE_LMMSE/MC;
TD_ChEstLI(ii)=TDMSE_LMMSE/MC;
TDD_ChEstALI(ii)=TDMSE_LMMSE/MC;
TDQabs_ChEstLI(ii)=TDQabsMSE_LMMSE/MC;
toc;
end

% Channel estimation

gridon;xlabel('SNR'); ylabel('Channel MSE');
semilogy(EbNodB,ChEst4PA,'k','LineWidth',2);
holdon
gridon;xlabel('SNR'); ylabel('Channel MSE');
semilogy(EbNodB,TD_ChEstLI,'g','LineWidth',2);
legend('4-Pilot Averaging','Linear Interpolation')
holdoff
figure
gridon;xlabel('SNR'); ylabel('Channel MSE');

```

```
semilogy(EbNodB,TDQabs_ChEstLI,'b','LineWidth',2);
holdon
gridon;xlabel('SNR'); ylabel('Channel MSE');
ThFS = (1/nFFT)*(beta./snr).*(1./(1+(beta./snr)));
semilogy(EbNodB,ThFS,'-.k','LineWidth',2);
legend('Linear Interpolation','Frequency Smoothing')
holdoff
holdoff
```